ACFI-T16-10

The Higgs Portal and Cosmology

Ketevi Assamagan,[a] **Chien-Yi Chen,**[b,c] **John Paul Chou,**[d] **David Curtin,**[e] **Michael A. Fedderke,**[f] **Yuri Gershtein,**[d] **Xiao-Gang He,**[g] **Markus Klute,**[h] **Jonathan Kozaczuk,**[i] **Ashutosh Kotwal,**[j] **Steven Lowette,**[k] **Jose Miguel No,**[l] **Tilman Plehn,**[m] **Jianming Qian,**[n] **Michael Ramsey-Musolf,**[o] **Alexei Safonov,**[p] **Jessie Shelton,**[q] **Michael Spannowsky,**[r] **Shufang Su,**[s] **Devin G. E. Walker,**[t] **Stephane Willocq,**[o] **Peter Winslow**[o]

[a] *Department of Physics, Brookhaven National Laboratory, Upton, New York, 11973*

[b] *Perimeter Institute for Theoretical Physics, Waterloo, ON N2L 2Y5, Canada*

[c] *Department of Physics and Astronomy, University of Victoria, Victoria, BC V8P 5C2, Canada*

[d] *Department of Physics and Astronomy, Rutgers University, 126 Frelinghuysen Road. Piscataway, NJ 08854-8019*

[b] *Maryland Center for Fundamental Physics, Department of Physics, University of Maryland, College Park, MD 20742-4111 USA*

[f] *Department of Physics and Kavli Institute for Cosmological Physics, The University of Chicago, Chicago, IL 60637, USA*

[g] *INPAC, SKLPPC, and Department of Physics, Shanghai Jiao Tong University, Shanghai, China*

[h] *Department of Physics, Massachusetts Institute of Technology, Cambridge, MA 02139 USA*

[i] *TRIUMF, 4004 Wesbrook Mall, Vancouver BC V6T 2A3, Canada.*

[j] *Department of Physics, Duke University,Physics Bldg., Science Dr., Durham, NC 27708 and Fermilab, Batavia IL 60510-5011*

[k] *Physics Department, Vrije Universiteit Brussel, Pleinlaan 2 — 1050 Brussel, Belgium*

[l] *Department of Physics and Astronomy, University of Sussex, Brighton, BN1 9QH, UK*

[m] *Institute for Theoretical Physics,Heidelberg University,Philosophenweg 16, 69120 Heidelberg, Germany*

[n] *Department of Physics, Randall Laboratory, University of Michigan, 450 Church Street, Ann Arbor, MI 48109-1040*

[o] *Amherst Center for Fundamental Interactions, Department of Physics, University of Massachusetts Amherst, Amherst, MA 01003 USA*

[p] *Department of Physics and Astronomy, Texas A & M University, College Station, TX 77843-4242*

[q] *Department of Physics, University if Illinois Urbana-Champaign, Urbana, IL 61801-3080*

[r] *Department of Physics, Durham University, South Road, Durham, DH1 3LE, UK*

[s] *Department of Physics, University of Arizona, Tucson, AZ 85721*

[t] *Department of Physics, University of Washington, Seattle, WA 98195, USA*

ABSTRACT: Higgs portal interactions provide a simple mechanism for addressing two open problems in cosmology: dark matter and the baryon asymmetry. In the latter instance, Higgs portal interactions may contain the ingredients for a strong first order electroweak phase transition as well as new CP-violating interactions as needed for electroweak baryogenesis. These interactions may also allow for a viable dark matter candidate. We survey the opportunities for probing the Higgs portal as it relates to these questions in cosmology at the LHC and possible future colliders.

Contents

1 Introduction

Explaining the origin and composition of the matter content of the Universe remains one of the most compelling tasks at the interface of high energy physics, nuclear physics, and cosmology. The identity of the dark matter that comprises 27% of the cosmic energy density remains undetermined, and little is known about its non-gravitational interactions. The visible matter comprises just under 5% of the present cosmic energy density and is often characterized by the baryon-to-photon ratio

$$Y_B = \frac{n_B}{s} = (8.59 \pm 0.11) \times 10^{-11} \tag{1.1}$$

where n_B (s) is the baryon number (entropy) density and where the value has been obtained from the Planck data[1]. This number, though tiny, is clearly decisive for the Universe as we know it, yet the Standard Model (SM) suggests it should be many orders of magnitude smaller. Thus, accounting for the abundance of both the visible and dark matter provides some of the strongest motivation for physics beyond the Standard Model (BSM).

It is possible that the dynamics associated with the dark matter and the origin of the baryon asymmetry are largely hidden from our view, either because the associated mass scale is too high or the relevant interactions with SM particles too feeble. In light of the discovery of the Higgs-like boson at the LHC, it is interesting to ask whether the properties and interactions of the Higgs boson provide a window, or "portal", on the origin and composition of the cosmic matter content. If so, what might one learn from more refined studies of Higgs boson properties and interactions at the LHC or from the search for additional Higgs-like states? The purpose of this document is to summarize the landscape of possibilities as reviewed at the workshop "Unlocking the Higgs Portal" held at the Amherst Center for Fundamental Interactions at the University of Massachusetts in May 2014[2]. In view of Run II of the LHC, it is particularly worthwhile to identify the Higgs boson properties and searches for new states that are most promising from the standpoint of the cosmic matter content problem. In what follows, we provide a snapshot of this landscape as well as a discussion of additional theoretical work needed to delineate the prospective consequences of future LHC studies. Given the prospects for developing the next generation of high energy colliders, we also discuss the prospective opportunities for probing cosmologically relevant Higgs portal scenarios at various new facilities under consideration, including the International Linear Collider (ILC), China Electron Positron Collider (CEPC) and Super Proton Proton Collider (SppC), and the CERN future circular colliders FCC-ee (electron-positron) and FCC-hh (proton-proton).

The collider phenomenology pertaining to dark matter has been extensively investigated, particularly in relation to the WIMP paradigm (see, *e.g.*, Refs. [3–5]). Dark matter-Higgs boson interactions have also been widely studied, and the high energy community is reasonably well versed in the dark matter problem (for recent discussions, see, *e.g.*. Refs. [6, 7]). The implications of present and future LHC studies for the origin of visible matter, on the other hand, is less widely appreciated. Consequently, in what follows we will place a somewhat heavier weight on the baryogenesis problem, linking it to the Higgs portal and dark matter relic abundance where appropriate. For completeness, we also provide a short summary of the collider phenomenology of Higgs portal dark matter.

In principle, the non-vanishing Y_B could have resulted from initial conditions during the Big Bang or from dynamics of grand unified theories at energy scales above $\sim 10^{16}$ GeV. In practice, the on-going success of the inflationary paradigm implies that any matter-antimatter asymmetry created in either of these ways would have been inflated away and, thus, not able to account for present observation. In this view, the particle physics of the post-inflationary

Universe (including the era of preheating) is likely responsible. Over 40 years ago, Sakharov[8] identified three ingredients in the early Universe that must have been present in order to generate a non-vanishing Y_B: (a) baryon number (B)-violation; (b) violation of both C- and CP-invariance; and (c) either a departure from equilibrium dynamics or violation of CPT-invariance. The SM contains the first ingredient in the form of (B+L)-violating sphaleron transitions, but fails on the second and third.

The possible BSM scenarios that satisfy all three "Sakharov" conditions span the gamut of post-inflationary cosmic history. Among the most theoretically attractive and experimentally testable are those that introduce new particles in the few-hundred GeV to TeV mass range. These scenarios would have generated the matter-antimatter asymmetry during or shortly before the era of electroweak symmetry-breaking (EWSB). The most thoroughly studied (though not exclusive) such scenario is electroweak baryogenesis (EWBG) (for a recent review, see Ref. [9]).

In EWBG, the Universe undergoes a first order phase transition during which electroweak symmetry is broken. The electroweak phase transition (EWPT) proceeds via nucleation of bubbles of broken electroweak symmetry as the Universe cools through a nucleation temperature T_N that lies below the phase transition critical temperature, T_C. This transition, which satisfies the Sakharov out-of-equilibrium condition, is analogous to the condensation of water droplets from vapor with decreasing temperature. Sakharov's second ingredient is provided by C- and CP-violating interactions of new particles at the bubble walls. These interactions ultimately induce the sphalerons to create baryons that diffuse inside the expanding bubbles where they are captured and protected from being washed out by inverse sphaleron processes.

The LHC and prospective future colliders are well-suited to looking for the particle physics ingredients needed for the first order EWPT. Indeed, the possibilities for generating this transition are rich. New particles may modify the Higgs potential through either loop effects or new tree level interactions. In some scenarios, the result may be new patterns of EWSB that would not arise in the Standard Model, such as the occurrence of a series of transitions that break SM symmetries. In all cases, the dynamics require the existence of new spin-zero particles whose interactions may be more or less analogous to those of the SM Higgs boson. If one (or more) of these new states is stable on cosmological time scales, it (they) may also account for the dark matter relic density. Alternatively, dark matter fields may interact with the new scalars that, in turn, interact with the SM through the Higgs portal.

Generically, we write the Higgs portal interaction as

$$\mathcal{L} \supset \frac{a_1}{2} H^\dagger \phi H + \frac{a_2}{2} H^\dagger H \phi^\dagger \phi + \cdots \quad , \tag{1.2}$$

where H is the SM Higgs doublet, ϕ is an additional scalar transforming as either a singlet or non-singlet under the SM, and the "$+ \cdots$" indicate possible higher dimensional operators. For the neutral component of ϕ to contribute to the dark matter relic density, the Z_2-odd terms in Eq. (1.2) must be absent (e.g., $a_1 \to 0$). On the other hand, ϕ may not itself be the dark matter candidate but may interact independently with the dark matter as in

$$\mathcal{L} \supset \bar{\chi} \left(a + b\gamma_5 \right) \phi\chi + \text{h.c.} + \cdots \quad , \tag{1.3}$$

where χ in this case is fermionic dark matter. The interactions (1.2,1.3) may provide the Higgs portal into the dark matter sector, while the operators in Eq. (1.2) may give rise for a strong first order EWPT as needed for EWBG.

The LHC and future colliders might discover the new particles (ϕ, χ) and probe the effects of their interactions in a number of ways:

- modified SM-like Higgs boson couplings to itself and other SM particles

- new Higgs boson production mechanisms

- new Higgs boson decay channels

- new scalar particles that interact with the Higgs boson and other SM particles

Many of these signatures have been discussed elsewhere in the literature. Here we discuss their relation to the possible occurrence of a first order EWPT and connection to dark matter, utilizing representative theoretical scenarios.

2 Theoretical Scenarios

The dynamics of the EWPT are governed by the finite-temperature effective action, $S_{\text{EFF}}(T)$, that reduces to an integral over the effective potential $V_{\text{EFF}}(\phi, T)$ for spatial homogenous background fields ϕ (here, we generically denote the full set of background fields by ϕ). For a theory such as the SM wherein only a single field acquires a vacuum expectation value (the background field), one may write the effective potential in the high-temperature limit

$$V_{\text{EFF}}(\varphi, T) = D(T^2 - T_0^2)\varphi^2 - (ET + e)\varphi^3 + \bar{\lambda}\varphi^4 + \cdots \quad , \tag{2.1}$$

where D, T_0^2, E, e, and $\bar{\lambda}$ are all computable from the zero temperature Lagrangian. In the SM, where φ is the Higgs background field (used here interchangeably with the vev), $\bar{\lambda}$ is approximately the Higgs self-coupling. The quantity DT^2 corresponds to the square scalar field thermal mass, while DT_0^2 is the zero temperature, tachyonic mass parameter, often denoted μ^2. The existence of the cubic term proportional to $ET + e$ is essential for the occurrence of a first order phase transition. In the SM, $e = 0$, as there exists no tree-level term that is cubic in the background field. In extended scalar sectors, e may be non-vanishing. The quantity E is generated at loop level in both the SM and its extensions.

The interplay between $(ET + e)$ and $\bar{\lambda}$ governs the character of the EWPT. In the limit that both E and e vanish, the transition becomes second order and no bubble nucleation will occur. The evolution of the potential with temperature for a first order EWPT is shown in Fig. 1. The first order transition is marked by the existence of a barrier between the unbroken ($\varphi = 0$) and broken ($\varphi \neq 0$) minima that requires $E > 0$ and/or $e > 0$. In a second order transition the cubic terms in the finite temperature potential do not appear.
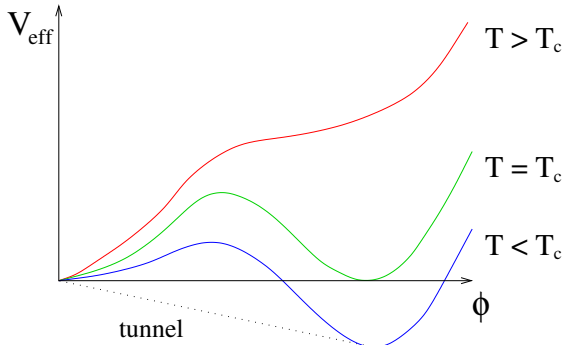
Figure 1. Evolution of the effective potential with T.

Assuming the occurrence of a first order transition with a sufficiently large bubble nucleation rate, preservation of any matter-antimatter asymmetry inside the bubbles requires quenching of the sphaleron transitions by making the sphaleron energy sufficiently large relative to the critical temperature, T_C. For the high-T potential of Eq. (2.1), the requirement becomes[10–12]

$$\frac{(ET_C + e)}{\bar{\lambda} T_C} \gtrsim 1 \quad . \tag{2.2}$$

This criterion is sometimes referred to as the requirement for a "strong first order EWPT" or "SFOEWPT". In the SM, for which $e = 0$ and E arises through loops, this criterion is

not satisfied, largely because the Higgs self coupling λ is too large, thereby suppressing the denominator in Eq. (2.2). Since $m_h^2 = \lambda v^2$, where v is the $T = 0$ vev, the requirement that the denominator of Eq. (2.2) be sufficiently small is equivalent to an upper bound on the Higgs boson mass. In fact, Monte Carlo studies indicate that the maximum Higgs boson mass for a first order EWPT in the SM is in the vicinity of 80 GeV[13–16], well below the observed value.

BSM scenarios may remedy the absence of a SFOEWPT by increasing the magnitude of E, reducing the magnitude of $\bar{\lambda}$, or reducing the critical temperature T_C. Broadly speaking, BSM scenarios do so *via* one or more of the following avenues:

- new loop effects that effectively increase E (Section 2.1)

- new tree-level interactions that generate non-vanishing e (Section 2.2)

- tree-level interactions that reduce $\bar{\lambda}$ either directly or indirectly (Section 2.2)

- tree-level or loop effects that lower the critical temperature, T_C (Section 2.2).

- new tree-level interactions that generate an earlier SFOEWPT along a different field direction, enabling EWBG through a multi-step process (Section 2.2)

2.1   Loop effects

The dynamics of a loop-induced SFOEWPT can be understood by considering the so-called "daisy resummation" contribution to $V_{\mathrm{EFF}}(\varphi, T)$. This contribution yields the following contribution to the difference in energy between the potential in the broken and unbroken phases:

$$\Delta V_{\mathrm{daisy}} = -\frac{T}{12\pi} \sum_k \left\{ \left[m_k^2 + y_k \varphi^2 + \Pi_k(T) \right]^{3/2} - \left[m_k^2 + \Pi_k(T) \right]^{3/2} \right\} \quad , \qquad (2.3)$$

where the sum is over all bosonic degrees of freedom with mass parameters m_k, couplings to the Higgs field y_k, and thermal masses $\Pi_k(T)$. The presence of $\Delta V_{\mathrm{daisy}}$ effectively generates a barrier between the two phases. For the transverse components of the W and Z bosons, both m_k^2 and $\Pi_k(T)$ vanish, leaving a pure $T\varphi^3$ term in the potential. The barrier can be increased by adding more scalar degrees of freedom and by choosing their mass parameters to roughly cancel the thermal contributions: $m_k^2 \sim -\Pi_k(T)$. Since the physical masses are given by $m^2 \sim m_k^2 + y_k v^2$, a SFOEWPT can lead to relatively light degrees of freedom at $T = 0$ under this scenario. The most widely studied example occurs in the MSSM (see, *e.g.* Ref. [17]), where the right-handed stop mass parameter is chosen to cancel its thermal mass,

leading to a stop that is lighter than the top quark. The effect is particularly important for stops, since they have large Yukawa couplings and introduce a factor of N_C when the sum in Eq. (2.3) is performed.

Searches for light stops at the LHC[18–22] as well as determinations of Higgs boson signal strengths[23, 24] appear to have closed most of the window for a SFOEWPT in the MSSM as well as extensions with hard SUSY-breaking terms. Going beyond SUSY, it was realized that loop contributions involving multiple species may also lower T_C in the presence of a barrier between the two phases[25]. When one of the $y_k < 0$, the corresponding contribution to ΔV_{daisy} will be positive, effectively increasing the energy of the broken phase relative to the unbroken phase. As a result, the Universe must cool to a lower temperature than it otherwise would for the two phases to be degenerate in energy, thereby leading to a lower T_C and increasing the left hand side of Eq. (2.3)[1].

Possible generation of a SFOEWPT through loop contributions has recently been studied in a general way by the authors of Ref. [26]. The introduction of colored scalar particles that lead to a SFOEWPT would also lead to significant increases in the hgg and $h\gamma\gamma$ couplings. Color singlets that are charged under the electroweak gauge groups and that give rise to a SFOEWPT would not modify the hgg coupling but could induce observable deviations in the rate for $h \to \gamma\gamma$. For gauge singlets that generate a SFOEWPT solely via loops rather than tree-level interactions (see below), one would expect a change in $\sigma(e^+e^- \to Zh)$. The projected sensitivity of the CEPC and FCC-ee could allow for an observation of these modifications of Higgs boson production and decays[2].

2.2 Tree-level interactions

The introduction of additional Higgs boson-scalar interactions leads to a number of possibilities for a SFOEWPT, including new patterns of EWSB where the occurrence of multi-step transitions to the present electroweak phase may entail such transitions. At the level of renormalizable operators, a broad range of possibilities are embodied in the Higgs portal interactions of Eq. (1.2).

The simplest scenario arises when ϕ is a real singlet, denoted here as S. At $T = 0$, the presence of the two operators in Eq. (1.2) implies the existence of two mass eigenstates

---

[1]Application of this idea to the stop and sbottom contributions to the effective potential and the implications for the EWPT are under investigation.

[2]We also note that loop effects arising from new degrees of freedom may modify the $T = 0$ potential in such a way that the SM gauge boson finite-temperature loops induce a SFOEWPT.

$h_{1,2}$ that are doublet-singlet mixtures[3]. For the dynamics of the transition, taking $a_1 < 0$, the cubic interaction introduces a tree-level barrier, generating a non-vanishing $e > 0$. The presence of a non-vanishing a_2 may lead to a reduction in the value of $\bar{\lambda}$ and a reduction in T_C. For $a_2 < 0$, one finds a direct reduction in $\bar{\lambda}$[11]. For positive a_2, the effect is indirect, involving the interplay of parameters in the scalar mass-squared matrix[27]. These features have been analyzed in a general fashion in Refs. [11, 27–30], while specific model realizations in the NMSSM have been studied in Refs. [31, 32].

For ϕ transforming non-trivially under $\mathrm{SU}(2)_L$, the constraints on the electroweak ρ-parameter imply that the vev of the neutral component of ϕ must be small at $T = 0$. As the latter is proportional to a_1, the corresponding tree-level barrier induced by non-vanishing a_1 between the symmetric and present electroweak vacua is too small to allow for a SFOEWPT at finite-T. On the other hand, for suitable choices of parameters, it is possible that electroweak symmetry breaks in two steps: (1) at temperature T_1, the neutral component of ϕ gets a vev while the doublet vev vanishes; (2) at $T_2 < T_1$, a second transition occurs to the vacuum with vanishingly small neutral ϕ vev and non-vanishing doublet vev. The first transition may be strongly first order, and in this phase sphaleron transitions are suppressed since ϕ transforms non-trivially under $\mathrm{SU}(2)_L$. The matter-antimatter asymmetry may be produced during this first step and preserved during the transition at T_2. A concrete realization of this possibility for ϕ being a real $\mathrm{SU}(2)_L$ triplet has been analyzed in Ref. [33, 34], while general considerations have been discussed in Ref. [35]. The vacuum structure of the potential and the two-step trajectory is illustrated in Fig. 2.

For the special case of the two Higgs doublet model (2HDM) where the ρ-parameter constraints do not apply to the vevs, initial studies by the authors of Refs. [36, 37] indicate that it is possible to achieve a SFOEWPT in a singlet step transition due to the presence of additional tree-level interactions involving the two doublets. The SFOEWPT-favored region of parameter space suggests that the neutral pseudoscalar A^0 should be moderately heavy and that it may be considerably heavier than the non-SM-like neutral scalar H^0.

Relaxing the requirement of renormalizability, the existence of higher-dimensional Higgs self-interactions may also enable a SFOEWPT during a singlet-step transition to the present electroweak vacuum[38–42]. Writing

$$V(H) = -\mu^2 H^\dagger H + \lambda (H^\dagger H)^2 + \eta (H^\dagger H)^3 + \cdots \quad . \tag{2.4}$$

----

[3]We will take h_1 to be the SM-like Higgs scalar.
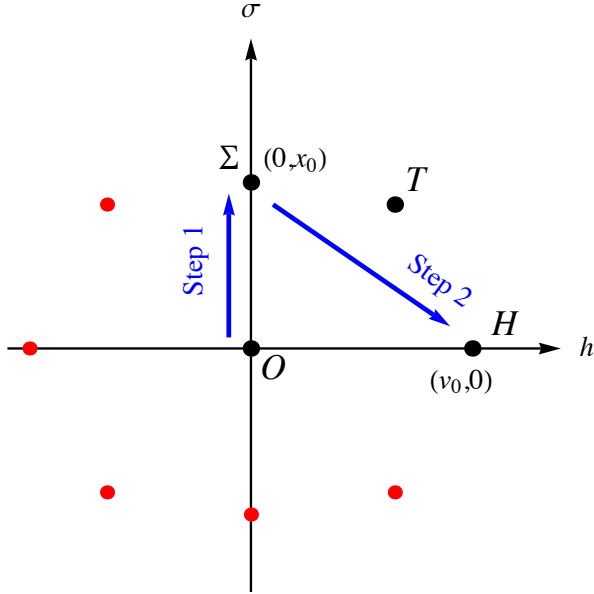
Figure 2. Two-step electroweak symmetry breaking for the real triplet Higgs portal scenario [33]. Here, h and σ denote the neutral Higgs boson and real triplet background fields, respectively; O gives the location of the symmetric phase, while Σ and H denote the locations of the triplet and Higgs phases, respectively. T indicates another extremal point, while the red points are related to the black points by Z_2 symmetries. The two step transition proceeds first along the triplet direction at a temperature T_σ, followed by a transition to the Higgs phase at a temperature $T_h < T_\sigma$.

one observes that when the dimensional parameter $\eta > 0$, the coefficient of the quartic self-coupling may be negative (subject to stability requirements), again introducing a tree-level barrier. This possibility may be particularly interesting when the Higgs is a pseudo-Goldstone boson, so that $\eta \sim 1/F_H^2$, with F_H being of order 100 GeV [39]. Alternately, when ϕ is a gauge singlet that is sufficiently heavy to be integrated out, a potential of the form in Eq. (2.4) may arise with $\lambda < 0$ and $\eta > 0$. For suitable choices of the singlet mass and couplings $a_{1,2}$, a SFOEWPT can be achieved. For related work on the EWPT treating the Higgs boson as a pseudo Goldstone Boson, see Ref. [39].

2.3 Higgs portal dark matter

The literature on dark matter is vast, and this short overview cannot do justice to the breadth of theoretical work that has been carried out on this subject. From a practical standpoint, we instead focus on a few representative cases that illustrate the features of Higgs portal interactions and that illustrate the phenomenological implications. We consider both scalar dark matter that may arise as part of an extended scalar sector and fermionic dark matter.

Scalar dark matter: gauge singlets. Extending the SM scalar sector with a real singlet S has been discussed above in the context of the EWPT. To achieve a viable dark matter candidate, the corresponding scalar potential must admit a Z_2 symmetry ($S \to -S$) that ensures stability of the S, with vanishing S vev at $T = 0$. The universe may still undergo a SFOEWPT to the EWSB Higgs vacuum if the singlet potential contains a tachyonic mass-squared term. In this case, the universe may first land in a vacuum with $\langle H^0 \rangle = 0$ and $\langle S \rangle \neq 0$ with decreasing T, followed by a transition to the $\langle H^0 \rangle \neq 0$ and $\langle S \rangle = 0$ vacuum at lower temperature [30]. For a non-tachyonic mass-squared term, a SFOEWPT is generally possible only when $\langle S \rangle \neq 0$ at $T = 0$. Avoidance of cosmic domain walls then implies that the potential must not be Z_2-symmetric, implying that $a_1 \neq 0$.

The general case (non-tachyonic mass) has been investigated by a number of authors[43–46]. In the standard thermal DM paradigm, the relic density is governed by the Higgs portal coupling a_2 that sets the strength of the annihilation channels $SS \to hh$ and $SS \to h \to f\bar{f}$ and VV. For m_S near $m_h/2$, the annihilation cross section σ_{ann} is dominated by single Higgs boson exchange (the "Higgs pole"), which is resonantly enhanced. The magnitude of a_2 must be accordingly reduced in order for the singlet density to saturate the observed DM relic density: $\Omega_S = \Omega_{DM}$. However, if the singlet constitutes one component of a multicomponent dark matter scenario, then one may have a larger magnitude for a_2 with $\Omega_S/\Omega_{DM} < 1$. Alternately, a non-thermal mechanism may lead to saturation of the observed relic density for larger a_2[47]. Note also that for the tachyonic mass scenario, stability of the Higgs/DM vacuum constrains the DM mass and relic density. The former is given by $-|\mu_s^2| + a_2 v^2$. The coupling a_2 must be positive and sufficiently large as to ensure a stable Higgs/DM vacuum. However, increasing a_2 leads to a smaller σ_{ann}. For a detailed study, see, *e.g.* Ref. [48].

DM direct detection experiments constrain the product $(\Omega_S/\Omega_{DM}) \times \langle \sigma_{\text{ann}} v \rangle$, v is the DM velocity. Constraints obtained including the recent LUX results are shown in Fig. 9 of Ref. [30] , assuming a thermal DM scenario. For non-thermal DM that yields $\Omega_S/\Omega_{DM} = 1$ the constraints are considerably more severe, except for m_S near $m_h/2$. The corresponding collider signatures are generally quite challenging (for a recent discussion, see, *e.g.*, Ref. [7]). Since $\langle S \rangle = 0$, the singlet cannot be produced directly in pp collisions as it does not mix with the SM Higgs boson and does not couple to any SM fields except pairwise to the Higgs boson. For $m_S \leq m_h/2$, the Higgs portal interaction a_2 leads to an invisible decay mode for the Higgs boson. The present LHC upper bound on the invisible branching fraction $\text{BR}(h \to \text{invis})$ is 23% [49, 50]. Note that this bound constrains the singlet fraction of the DM relic density

from being arbitrarily small, since $|a_2|$ cannot be arbitrarily large. For $m_S > m_h/2$, S is pair produced only through off-shell Higgs boson processes that have a relatively small cross section.

Variants on the simplest scenario of the SM plus a real singlet include extending the SM with a complex singlet[51–53] and extending the 2HDM with a real singlet[44, 54]. As discussed in Ref. [51] for the complex singlet $\mathbb{S}$, it is convenient to assign to the singlet field a global U(1) charge. For a U(1) conserving potential, $\mathbb{S}$ is equivalent to two degenerate real singlets that behave much like the real singlet as a dark matter candidate. Introducing U(1)-breaking into the potential then splits the masses of the two components of $\mathbb{S}$, yielding a two-component DM scenario. The relative contributions of each to the relic density depend on the mass splitting and the magnitude of the singlet quartic self coupling. If $\langle \mathbb{S} \rangle \neq 0$, then the Goldstone boson of the spontaneously broken U(1) will be stable. Explicitly breaking the U(1) makes this field a massive, viable DM candidate. The remaining degree of freedom associated with $\mathbb{S}$ then behaves like the real singlet that mixes with the SM Higgs boson. The resulting two mass eigenstates then appear as s-channel poles in the DM annihilation amplitude. The DM direct and indirect detection signatures, as well as the collider phenomenology, entails a combination of those associated with the real singlet when it is either a DM candidate or unstable. Under this scenario, one may also encounter a SFOEWPT. As also noted in Ref. [51], the presence of the complex scalar then allows for complex couplings in the potential as well as a situation in which both components of the scalar receive vevs, a feature that would generally preclude the existence of a viable DM candidate. However, if that situation is associated with the first step of a two-step EWPT, and if it goes to zero during the second transition to the SM vacuum, then one (or more) of the components of $\mathbb{S}$ may remain stable at and below the freeze-out temperature for thermal DM[53].

Another variant on the simplest scenario of the SM plus a real singlet has been studied recently in Refs. [44, 54] using a 2HDM plus a real singlet. Generically, the presence of a second neutral CP-even Higgs state opens up the parameter space of Higgs portal couplings that is consistent with the observed relic density. For low values of m_S, the annihilation rate to $b\bar{b}$ can be enhanced for large $\tan\beta$ in the Type II 2HDM, further opening the available parameter space, thereby allowing for a value of a_2 consistent with direct detection constraints and while achieving the observed relic density[54].

Non-singlet scalar dark matter: minimal dark matter. When ϕ carries SM gauge

charges and has integer isospin, the neutral component ϕ^0 may be a viable DM candidate. A similar situation holds for one of the neutral states in a 2HDM. Stability of ϕ^0 requires a $\mathbb{Z}_2$ symmetry, which must either be imposed by hand for lower dimensional representations of $SU(2)_L$ or is automatic for higher dimensional representations. The latter situation generally corresponds to "minimal dark matter" [55, 56]. In order to evade DM direct detection limits, scalar dark matter must either have zero hypercharge or a highly suppressed coupling to the Z^0 boson; otherwise, the DM-nucleus neutral current scattering cross section will lie well above present direct search bounds.

A general study of non-singlet scalar DM has been carried out in Ref. [57]. These authors found that the both the $\mathbb{Z}_2$ symmetric 2HDM and both the real or complex scalar multiplets of dimension $n = 3$, 5, or 7 may be viable. The lower bounds on the corresponding masses range from roughly 500 GeV to 20 TeV depending on n and assuming saturation of the relic density. A detailed study of the collider phenomenology for the real $n = 3$ case has been carried out in Ref. [58]. In general one would search for one or more disappearing charged particle tracks when one or more charged states is produced through electroweak pair production. Results of a CMS search for disappearing charged particle tracks are reported in Ref. [59]. For neutralinos in the MSSM under the anomaly mediated SUSY-breaking scenario, a neutralino with mass less than 260 GeV is excluded. One might anticipate a similar bound for the scalar DM scenarios, though to our knowledge none has yet been reported in the literature. For the real triplet of Ref. [58], saturation of the full relic density requires a DM mass at or above roughly 2 TeV, well above the present CMS exclusion. Note that in the two-step EWPT scenario described earlier (see Sec. 2.2), the CMS exclusion would likely preclude a stable neutral triplet in the minimal version of this scenario.

Fermionic dark matter. In general, a Higgs portal interaction with one or more additional fermionic multiplets χ may provide for a viable fermionic DM scenario, though it will not substantially affect the EWPT. On the other hand such an interaction may provide for new sources of CPV as needed for EWBG during a SFOEWPT, a possibility that has been analyzed recently in Refs. [60, 61] but that we will not explore in detail here. For the simplest, pure DM scenario, one introduces a non-renormalizable interaction of the form

$$\mathcal{L} \supset \frac{1}{\Lambda} H^\dagger H \left(\cos \xi \, \bar{\chi}\chi + \sin \xi \, \bar{\chi} i \gamma_5 \chi \right) \tag{2.5}$$

where χ is a SM gauge singlet and Λ defines an effective mass scale that incorporates the values of the scalar and pseudoscalar operator coefficients up to their relative normalization.

A detailed study of this scenario has been carried out in Ref. [62]. Saturation of the relic density requires Λ to range from a few hundred GeV to a few TeV, while constraints on the Higgs boson invisible width impose a strong exclusion for $m_\chi < m_h/2$. Unitarity constraints on an extension of the simplest scenario that includes both the SM Higgs boson and a real scalar singlet have been studied in Ref. [63]. Generation of the baryon asymmetry in a 2HDM variant of the interaction (2.5) has been studied in Ref. [61].

Portal to a hidden sector. Dark matter particles may exist in a hidden sector containing additional degrees of freedom that may couple to the Higgs boson. If these degrees of freedom are sufficiently light, they may significantly affect dark matter dynamics, leading, for example, to an enhanced annihilation cross section. A particularly interesting possibility is that the hidden sector contains a U(1) symmetry that is spontaneously broken. The corresponding massive gauge boson X may mix with the SM hyper charge boson, leading to the existence of an additional "dark photon" or "dark Z", Z_D. Alternately, the hidden sector may contain one or more SM gauge singlet scalars S that couple to the X. As discussed in Section 2.2, Higgs portal interactions of the form (1.2) will lead to h-S mixing. In this context, the Higgs-like state h_1 will inherit the couplings of S to X, albeit suppressed by the mixing angle $\sin\theta$. For Z_D mass below $m_h/2$, this scenario leads to the exotic Higgs decay $h_1 \to Z_D Z_D$. The corresponding phenomenology for this possibility has been extensively analyzed in Ref. [64]. Rather than repeat that discussion here, we refer the reader to that work.

A summary of various scenarios is given in Table 1.

3   Signatures and Benchmarks

Because the nature of an EWPT depends critically on the interactions of new particles with the Higgs doublet, measuring the Higgs boson properties, including its self-interactions as well as interactions with other SM particles through production and decays can provide a probe of phase transition dynamics. In addition, it is possible to search for the new degrees of freedom through their direct production. Thus, the scenarios for baryogenesis-favorable phase transitions summarized in Section 2 may lead to a number of signatures accessible at the LHC and prospective future colliders. For each of the simplest Higgs portal scenarios, the possibilities are indicated in the last column of Table 1. We also indicate which scenarios may allow for a viable dark matter candidate and indicate some of the corresponding signatures.

In what follows, we summarize work completed to date on some of these prospective signatures, followed by a brief roadmap for future analyses.

3.1 Modified Higgs self-coupling

In the real singlet Higgs portal scenario, the Higgs cubic self interaction $\lambda v h^3$ becomes $g_{111} h_1^3$, where g_{111} is a combination of the potential parameters, v, and the singlet vev. The value of this coupling can provide a probe of a SFOEWPT[26, 27, 65]. As shown in Fig. 3, the value of g_{111} is strongly correlated with T_C, with smaller g_{111} corresponding to lower critical temperature[27]. Moreover, its value may be considerably less than its pure SM value ~ 30 GeV, thereby allowing for rather low transition temperatures. A measurement of g_{111} can, thus, provide a probe of T_C and the SFOEWPT-viable regions of singlet extensions. Speaking conservatively, one expects a $\sim 30-50\%$ determination of this parameter at the HL-LHC[66–68]. Current projections for the ILC anticipate a 27% and 16% (10%) determination using the full data set at $\sqrt{s} = 500$ GeV and 2(5) ab^{-1} at 1 TeV respectively, considering the $4b$ and $bbWW$ final states[69]. Expectations next generation pp colliders vary. Refs. [70, 71] project, respectively a 40% and 30% determination with 4 ab^{-1} and 3 ab^{-1} at $\sqrt{s} = 100$ TeV, implying on the order of a 10% determination with 30 ab^{-1}. For center of mass energies below the di-Higgs production threshold, as would be relevant for the future circular e^+e^- colliders, one may determine g_{111} indirectly as it contributes to associated production at one-loop order[72, 73]. A 30% determination may be possible with this approach.
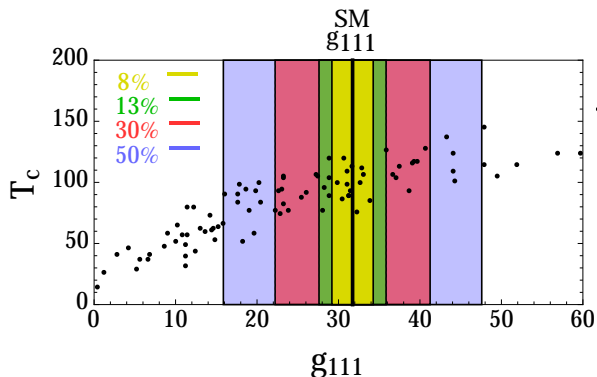
Figure 3. Correlation between the critical temperature and SM-like Higgs scalar self-coupling in the singlet-extended SM, adapted from Ref. [27]. Colors indicate future sensitivities of the HL-LHC (purple), CEPC/FCC-ee (red), ILC (green), and SPPC/FCC-hh (yellow).

3.2 Modified Higgs boson couplings to SM particles

The aforementioned scenarios may lead to changes in the Higgs boson couplings to other particles through the effect of Higgs mixing and/or new loop contributions. In the case of doublet-singlet mixing, for example, the SM-like state h_1 and singlet-like state h_2 may be written as

$$h_1 = h\cos\theta + S\sin\theta$$
$$h_2 = h\sin\theta - S\cos\theta \quad , \tag{3.1}$$

where $|\cos\theta| \geq 1/\sqrt{2}$. In the regime $m_2 > m_1/2$, the SM-like Higgs boson has no new decays and its branching ratios are unchanged from the SM. However, the production cross section, and thus, signal strength, will be reduced by $\cos^2\theta$. Present LHC data imply $\cos^2\theta \gtrsim 0.71$[27], a bound expected to increase to ~ 0.95 with the HL-LHC. Figure 4 shows the distribution of parameter space points for a SFOEWPT transition in the $\cos\theta$-m_2 plane for $2m_1 > m_2 > m_1/2$. One sees that for EWPT-viable regions of parameter space, there exist considerable possibilities for future precision Higgs boson studies to observe deviations from signal strengths expected for a purely SM Higgs boson. Some of this parameter space may be probed with the HL-LHC. A circular e^+e^- Higgs factory, such as the CEPC or FCC-ee, could allow a probe at better than one percent, and we see that there exist many SFOEWPT-viable models that would correspond to mixing of this magnitude or smaller.

For the case where the singlet generates the SFOEWPT solely via loop effects, one may expect an observable reduction in the associated production cross section $\sigma(e^+e^- \to Zh)$ of more than 0.4% . This possibility is illustrated in Fig. 5, where the dashed lines indicate the relative change in the associated production cross section and the solid lines indicate the value of the RHS of Eq. (2.2). In the regions where the RHS is $\gtrsim 1$, the reduction in $\sigma(e^+e^- \to Zh)$ is expected to be large enough to be observed at the CEPC or FCC-ee.
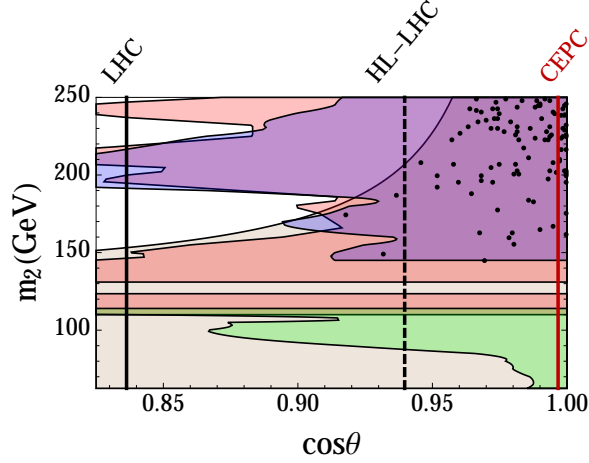
When the singlet mass m_S parameter is heavy ($m_S >> m_h$), one may integrate out the singlet degrees of freedom, thereby generating the higher dimension operators[41, 74]

$$\mathcal{O}_H = \frac{1}{2}\left(\partial_\mu H^\dagger H\right)^2 \tag{3.2}$$
$$\mathcal{O}_6 = (H^\dagger H)^3 \quad . \tag{3.3}$$

The resulting contribution to the Lagrangian will be

$$\mathcal{L}_{\text{eff}} \supset \frac{a_1^2}{m_S^4}\mathcal{O}_H - \left(\frac{a_1^2 a_2}{m_S^4} - \frac{2a_2^3 b_3}{m_S^6}\right)\mathcal{O}_6 \tag{3.4}$$

Figure 4. Correlation between the singlet-like Higgs boson mass m_2 and doublet-singlet mixing angle θ in the singlet-extended SM for $m_1 = 125$ GeV, adapted from Ref. [27]. Black points indicate SFOWEPT-viable models that also satisfy electroweak precision constraints. Colors regions indicate allowed regions from various Higgs boson measurements, heavy Higgs searches, and electroweak precision constraints as discussed in Ref. [27]. Vertical lines indicate mixing angle sensitivities of the present LHC combined fit results and prospective future HL-LHC and CEPC sensitivities. The latter have been obtained assuming a similar sensitivity as would be obtained at the FCC-ee (TLEP 240) collider.
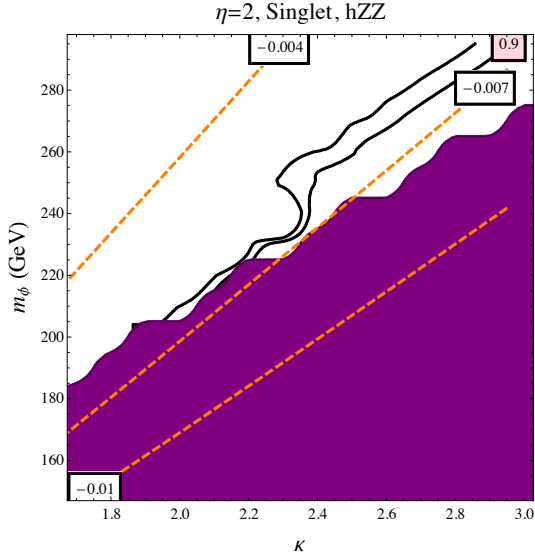
Figure 5. Correlation between SFOEWPT and $\sigma(e^+e^- \to Zh)$ for the singlet extension of the Standard Model[26] in the singlet mass-Higgs portal coupling plane. Dashed red lines correspond to relative changes in $\sigma(e^+e^- \to Zh)$. Solid lines give values of the LHS of Eq. (2.2). Purple gives region of non-vanishing singlet vev.
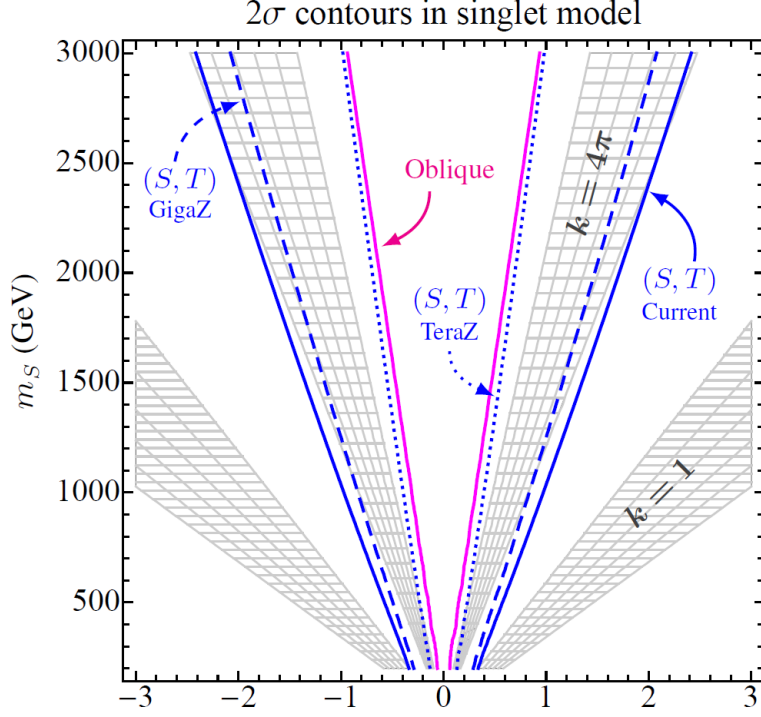
Figure 6. 2σ Contours of future precision measurements for a heavy singlet-catalyzed EWPT[41] in the $(a_1/m_S, m_S)$ plane. The magenta contour is the 2σ sensitivity to the universal Higgs oblique correction entering associated production at the ILC 500up. Blue contours show the 2σ RG-induced constraints from the S and T parameters from current measurements (solid) and future sensitivities at ILC GigaZ (dashed) and TLEP TeraZ (dotted). Regions of a viable first order EWPT, from Eq. (3.6), are shown in the gray, hatched regions for $k \equiv a_2 = 1$ and 4π. Figure courtesy of the authors of Ref. [41].

where $b_3/3$ is the singlet cubic self coupling. The resulting universal Higgs coupling correction is

$$\delta Z_h = \frac{2v^2 a_1^2}{m_S^4} \tag{3.5}$$

independent of the quartic Higgs portal coupling a_2. On the other hand, both the cubic and quartic portal couplings can enable SFOEWPT if

$$\frac{2v^4}{m_H^2} < \frac{m_S^2}{a_1^2 a_2} < \frac{6v^4}{m_H^2} \quad . \tag{3.6}$$

The resulting constraints on the (a_1, m_S) parameter space for different representative choices for a_2 are shown in Fig. 6. The gray regions correspond to a SFOEWPT for different representative values of a_2. The region below the pink solid lines could be probed with the measurement of $\sigma(e^+e^- \to Zh)$ at the CEPC/FCC-ee. Additional constraints arising from present and possible future electroweak precision tests are induced by the blue lines.

For the Higgs portal scenarios involving $SU(2)_L$ non-singlet representations ϕ, loop contributions may also lead to modified Higgs boson couplings to SM particles. If ϕ is an $SU(3)_C$ singlet, one will expect no modification of the gluon fusion operator $H^\dagger H G G$, but new contributions to the rate for $h \to \gamma\gamma$ will appear whose impact will depend on the magnitude and sign of a_2 and the ϕ mass. For the real triplet illustration, the correlation between the relative change in $\Gamma(h \to \gamma\gamma)$, the values of a_2 and the triplet mass, and the occurrence of a two-step transition are shown in Fig. 7. One finds that the existence of the two-step transition generally implies a reduction in the Higgs diphoton decay rate. With the HL-LHC, the CMS collaboration projects a probe of the diphoton signal strength with 2% precision[75], while ATLAS projects at least a 5% determination[76]. Combining the projected LHC determination of the ratio of branching ratios $\mathrm{BR}(h \to \gamma\gamma)/\mathrm{BR}(h \to ZZ)$ with the precise determination of the ZZh coupling at the ILC would allow a one percent determination of the Higgs diphoton coupling[69]. The present CEPC projection is for a 4.7% determination of the coupling with 5 ab^{-1} integrated luminosity[77], while for the FCC-ee one anticipates 3% determination of the signal strength with associated production and 10 ab^{-1} of data[78]. Determinations at this level of precision would provide a decisive test of the simplest realization of the multi-step transition paradigm.

3.3 Exotic Higgs boson Decays

The discovery of non-standard (exotic) Higgs boson decays as well as of non-SM Higgses could provide important information about Higgs portal interactions. As indicated above,

m_H=125 GeV, b_4=0.75

200
10% 3% 0% (SM) -3% -10%
180
20%
160
-20%
140 35%
m_Σ (GeV)
120 -35%
100
80
-2 -1 0 1 2
a_2
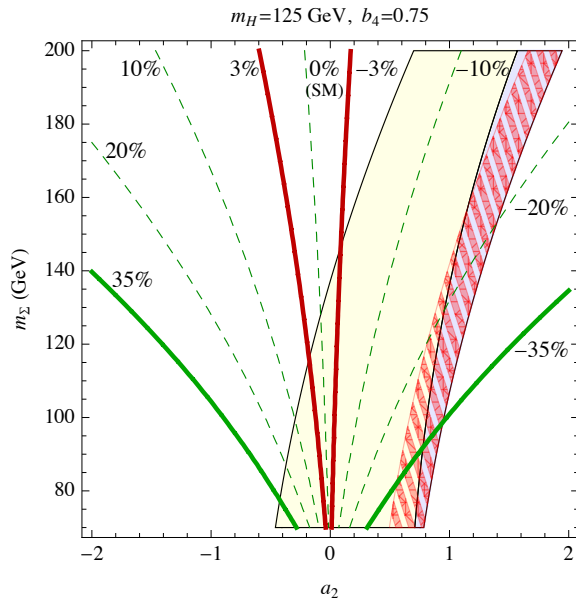
Figure 7. Shift in $\Gamma(h \to \gamma\gamma)$ in the real triplet extended SM [33]. The red hatched region corresponds to a two-step phase transition. Dashed curves indicate relative changes in $\Gamma(h \to \gamma\gamma)$ compared to its Standard Model value. Solid green and red curves correspond to relative shifts of $\pm 35\%$ and $\pm 3\%$, respectively. Figure courtesy of H. Patel.

the decay $h \to Z_D Z_D$ would signal the presence of a new dark sector containing a SM gauge singlet scalar and a U(1)$'$ gauge boson[64]. For $m_S < m_h/2$, the SM Higgs boson may decay invisibly to a pair of S bosons. In the absence of h-S mixing, this decay mode will correspond to an invisibly decaying Higgs boson, whereas in the presence of h-S mixing the final states will involve pairs of SM Higgs boson decay final states.

For the non-SM neutral Higgses, which appear in the new physics models with an extended Higgs sector, most of the current searches at the LHC focus on the conventional Higgs boson search channels of WW, ZZ, $\gamma\gamma$, $\tau\tau$ and bb channel [79–88]. The production of the extra Higgses is usually suppressed compared to that of the SM Higgs boson, either due to its larger mass or its suppressed couplings to the SM particles. The decay of the heavy neutral Higgses to the WW and ZZ final states is absent for the CP-odd Higgs boson, and could be highly suppressed for the non-SM like CP-even Higgs boson. The decay modes of $\tau\tau$ or bb suffer from either suppressed signal or large SM backgrounds, and are therefore only relevant for regions of the parameter space with an enhanced bb or $\tau\tau$ coupling. The search for the charged Higgs bosons at the LHC is even more difficult. For $m_{H^\pm} > m_t$, the cross section for the dominant production channel of $tbH^\pm$ is typically small. The dominant decay mode

$H^\pm \to tb$ is hard to identify given the large tt and $ttbb$ background, while the subdominant decay of $H^\pm \to \tau\nu$ has suppressed branching fraction. In the MSSM, even at the end of the LHC running, there is a "wedge region" [89] in the $m_A - \tan\beta$ plane for $\tan\beta \sim 7$ and $m_A \gtrsim 300$ GeV in which only the SM-like Higgs boson can be covered at the LHC. Similarly, the reach for the non-SM Higgses is limited in models with an extended Higgs sector.

In addition to their decays to the SM particles, non-SM Higgses can decay via exotic modes, *i.e.*, heavier Higgs decays into two light Higgses, or one light Higgs boson plus one SM gauge boson. Five main exotic decay categories for Higgses of the Type II 2HDM are shown in Table 2. These channels typically dominate once they are kinematically open. A recent study on exotic Higgs boson decays can be found in Refs. [90–101].

Note that most of the current experimental searches for the non-SM Higgs boson assume the absence of exotic decay modes. Once there are light Higgs states such that these exotic modes are kinematically open, the current search bounds can be greatly relaxed given the suppressed decay branching fractions into SM final states [91, 93, 95]. Furthermore, exotic Higgs decays to final states with two light Higgses or one Higgs boson plus one SM gauge boson provide complementary search channels. Here, we list such exotic Higgs decays and consider potential search strategies.

- $H^0 \to AA$ or $H^0 \to h^0 h^0$

With the final state Higgs boson decaying via bb, $\gamma\gamma$, $\tau\tau$, WW^*, final states of $bbbb$, $bb\tau\tau$, $bb\gamma\gamma$ and $\gamma\gamma WW^*$ can be used to search for resonant Higgs boson decay to two light neutral Higgses. Current searches at the LHC 8 TeV with about 20 fb^{-1} luminosity observed 95% C.L. cross section limits of 2.1 pb at 260 GeV and about 0.018 pb at 1000 GeV [102] (see also Refs. [103–105]). While $bb\gamma\gamma$ and $bb\tau\tau$ have comparable sensitivities at low mass, the $bbbb$ mode dominates at high mass.

- $H^0 \to AZ$ or $A \to H^0 Z$

With $Z \to \ell\ell$ and $H^0/A \to bb, \tau\tau$, the final states of $bb\ell\ell$, $\tau\tau\ell\ell$ can be obtained with gluon fusion production, or in the bb associated production with two additional b jets [90–92]. Recent searches from ATLAS and CMS have shown certain sensitivity in this channel [83, 106–109]. In parameter regions where $\mathrm{Br}(A \to H^0 Z) \times \mathrm{Br}(H^0 \to ZZ)$ is not completely suppressed, ZZZ final states with two Z decaying leptonically and one Z decaying hadronically can also be useful [91]. Other channels with top final states could be explored as well.

Note that the decay $A \to ZH^0$ has been identified as a particular signature of a SFOEWPT in the 2HDM[36]. As discussed below, the prospects for observing this channel in the $\ell\ell b\bar{b}$ and $\ell\ell W^+W^-$ model have been analyzed in Ref. [37].

- $H^0 \to H^+H^-$

With both $H^\pm$ decaying via $\tau\nu$ final states, the signal of $\tau\tau\nu\nu$ can be separated from the SM W^+W^- background since the charged tau decay product in the signal typically has a hard spectrum compared to that of the background [95].

- $H^0/A \to H^\pm W^\mp$

Similar to the H^+H^- case, $H^\pm \to \tau\nu, tb$ and $W \to \ell\nu$ with $\ell\tau\nu\bar{\nu}$ or $tb\ell\nu$ could be used to search for $H^0/A \to H^\pm W^\mp$. Note that for the CP-even Higgs boson H^0, the branching fraction of $H^0 \to H^\pm W^\mp$ is mostly suppressed comparing to $H^0 \to H^+H^-$ as long as the latter process is kinematically open and not accidentally suppressed [95]. However, for the CP-odd Higgs boson A, this is the only decay channel with a charged Higgs boson in the decay products.

- $H^\pm \to H^0 W^\pm, AW^\pm$

This is the only exotic decay channel for the charged Higgs boson in the 2HDM. Given the associated production of $tbH^\pm$, and the decay of H^0, A into the bb or $\tau\tau$ channel, $\tau\tau bbWW$ or $bbbbWW$ can be used to probe this channel [93]. $H^0/A \to t\bar{t}$ could also be used given the boosted top in the high energy environment.

Note that while $H^\pm \to WZ$ is absent in 2HDM type extension of the SM Higgs sector, it could appear, however, in the real triplet models extension of the SM once the triplet obtains a vev [58].

- $A/H^0 \to tt$, $H^\pm \to tb$

While $A/H^0 \to tt$ and $H^\pm \to tb$ are considered to be challenging experimentally, a recent study of BSM Higgs searches with top quarks in the final states [110] showed that a combination of the channels of $pp \to bbH^0/A \to bbtt, bb\tau\tau$, $pp \to H^0/A \to tt$ as well as $pp \to tbH^\pm \to tbtb, tb\tau\nu$ yields full coverage for $\tan\beta$ and pushes the exclusion limits from the $\mathcal{O}(1)$ TeV at the LHC to the $\mathcal{O}(10)$ TeV at a 100 TeV pp collider.

3.4 New states

In addition to observing deviations of Higgs boson couplings to SM particles, one may also anticipate direct production of new states associated with SFOEWPT-viable models. Again, the singlet scenario provides the simplest illustration. Its production cross section will be proportional to $\sin^2\theta$, presently constrained to be smaller than ~ 0.34. For $m_2 < 2m_1$, the signatures of this state would be identical to those of a SM Higgs boson with reduced signal strength[4]. For $m_2 > 2m_1$, where m_1 is the mass of the SM-like Higgs boson, a new decay mode $h_2 \to h_1 h_1$ becomes kinematically allowed, introducing the possibility of resonant di-Higgs production. The final states would entail pair-wise combinations of SM Higgs boson decay products, such as $b\bar{b}\gamma\gamma$, $b\bar{b}\tau^+\tau^-$ etc.. Recently, the authors of Ref. [111] showed that observation of resonant di-Higgs production in the $b\bar{b}\tau^+\tau^-$ channel – the same one discussed in Ref. [112] for non-resonant production to determine the self-coupling – could be feasible with 100 fb^{-1} at the LHC, assuming the present maximal value of 0.34 for $\sin^2\theta$. Other studies have analyzed resonant di-Higgs production with $b\bar{b}\gamma\gamma$ and $4b$ final states, though not with an eye toward the EWPT [113–115]. Looking to the future, should the constraints on the mixing angle become more severe, higher integrated luminosity, a cleaner background environment, or higher parton luminosity as with the SPPC/FCC-hh would be needed to search for such modes.

For non-singlet ϕ, such as the real triplet (Σ) or 2HDM discussed above, production and decays provide for a rich phenomenology. The electroweak ρ-parameter constraints on the non-doublet vevs imply that single scalar production is typically suppressed, and the dominant production mechanism will be electroweak pair production. For multi-Higgs doublet models, on the other hand, neutral scalars may be produced through gluon fusion, while charged states may be singly-produced through associated production. The final states in regions of interest for cosmology will then depend on the details of each scenario.

Two Higgs doublets. For the 2HDM, the authors of Ref. [37] have shown that in the SFOEWPT-viable region of parameter space, the decay $A^0 \to ZH^0$ could be discovered at the 14 TeV LHC in the $\ell\ell b\bar{b}$ and $\ell\ell W^+W^-$ channels with integrated luminosity in the $\gtrsim 20 - 40$ fb^{-1} range. Analyses of decays involving charged scalars $H^\pm$ remain to be performed.

Real triplet. For vanishing triplet vev, the neutral component may contribute to the DM relic

---

[4]Recall that the mixing angle cancels from the branching ratios when no new decay channels are kinematically allowed.

density. For masses in the several hundred GeV range, where the two step phase transition appears to be viable, the triplet contribution will comprise less than 10% of the relic density due to the sizable cross section for annihilation into W^+W^- pairs. At the LHC, triplet states are produced electroweakly in $\Sigma^+\Sigma^-$ and $\Sigma^\pm\Sigma^0$ pairs. Electroweak radiative corrections raise the $\Sigma^\pm$ masses relative to the Σ^0 mass by ~ 160 MeV, so that the $\Sigma\pm$ may decay to a Σ^0 plus a soft pion or lepton-neutrino pair. None of the SM final state particles will be detectable. The signature would, thus, be large $\not{E}_{\mathrm{T}}$ plus one or more disappearing charged particle tracks. For a 150 GeV Σ^+ the $c\tau$ is of order 5 cm[58]. The prospective implications of the CMS search for disappearing charged particle tracks[59] have been discussed above in Section 2.3.

For non-vanishing vev, both the neutral and charged triplet can decay, leading to a rich array of possible final states[58]. For $\Sigma^\pm$ masses well below the $W^\pm Z$ threshold, the dominant decay mode is $\tau\nu$ when the triplet vev is of order one GeV, while it is Σ^0 plus a soft pion for very small vev. The largest Σ^0 branching fraction is to $b\bar{b}$. Thus, one may anticipate $b\bar{b}\tau\nu$ final states for the first case and $b\bar{b}\gamma\gamma$ or $b\bar{b}\tau^+\tau^-$ for the second. In the study of Ref. [111], it was found that a discovery with the $b\bar{b}\tau\nu$ channel may be possible with 100 fb^{-1} at the 14 TeV LHC, with a significance depending on the magnitude and sign of the Higgs portal coupling a_2 and the triplet mass. Correlating this observation with the SM-like Higgs boson diphoton branching fraction, as discussed above, could indicate the presence of the real triplet with SFOEWPT-favorable parameters.

4   Future Work

It is clear that there exists a rich set of experimental signatures of the Higgs portal in cosmologically-relevant regions of parameter space. While detailed studies have been carried out for a subset of these signatures, substantial additional work is called for. In Table 3 below, we summarize the landscape of completed and prospective studies. From both this discussion and Table 3 we see that there exist considerable opportunities for both new experimental searches and theoretical studies. As the theoretical work develops, we will periodically up-date this document to reflect new results. We also point to a companion document that summarizes the outcome of a recent ACFI workshop "Probing the Electroweak Phase Transition with a 100 TeV pp Collider" that was held at the University of Massachusetts Amherst in September 2015.

5 Acknowledgements

References

[1] PLANCK collaboration, P. Ade et al., *Planck 2013 results. XVI. Cosmological parameters*, *Astron.Astrophys.* (2014) , [1303.5076].

[2] "ACFI Workshop Unlocking the Higgs Portal." http://www.physics.umass.edu/acfi/seminars-and-workshops/unlocking-the-higgs-portal.

[3] D. E. Morrissey, T. Plehn and T. M. P. Tait, *Physics searches at the LHC*, *Phys. Rept.* **515** (2012) 1–113, [0912.3259].

[4] J. Abdallah et al., *Simplified Models for Dark Matter Searches at the LHC*, *Phys. Dark Univ.* **9-10** (2015) 8–23, [1506.03116].

[5] D. Abercrombie et al., *Dark Matter Benchmark Models for Early LHC Run-2 Searches: Report of the ATLAS/CMS Dark Matter Forum*, 1507.00966.

[6] J. Abdallah et al., *Simplified Models for Dark Matter and Missing Energy Searches at the LHC*, 1409.2893.

[7] N. Craig, H. K. Lou, M. McCullough and A. Thalapillil, *The Higgs Portal Above Threshold*, 1412.0258.

[8] A. Sakharov, *Violation of CP Invariance, c Asymmetry, and Baryon Asymmetry of the Universe*, *Pisma Zh.Eksp.Teor.Fiz.* **5** (1967) 32–35.

[9] D. E. Morrissey and M. J. Ramsey-Musolf, *Electroweak baryogenesis*, *New J.Phys.* **14** (2012) 125003, [1206.2942].

[10] M. Quiros, *Finite temperature field theory and phase transitions*, in *High energy physics and cosmology. Proceedings, Summer School, Trieste, Italy, June 29-July 17, 1998*, pp. 187–259, 1999. hep-ph/9901312.

[11] S. Profumo, M. J. Ramsey-Musolf and G. Shaughnessy, *Singlet Higgs Phenomenology and the Electroweak Phase Transition*, *JHEP* **0708** (2007) 010, [0705.2425].

[12] H. H. Patel and M. J. Ramsey-Musolf, *Baryon Washout, Electroweak Phase Transition, and Perturbation Theory*, *JHEP* **1107** (2011) 029, [1101.4665].

[13] M. Gurtler, E.-M. Ilgenfritz and A. Schiller, *Where the electroweak phase transition ends*, *Phys. Rev.* **D56** (1997) 3888–3895, [hep-lat/9704013].

[14] M. Laine and K. Rummukainen, *What's new with the electroweak phase transition?*, *Nucl. Phys. Proc. Suppl.* **73** (1999) 180–185, [hep-lat/9809045].

[15] F. Csikor, Z. Fodor and J. Heitger, *Endpoint of the hot electroweak phase transition*, *Phys. Rev. Lett.* **82** (1999) 21–24, [hep-ph/9809291].

[16] Y. Aoki, F. Csikor, Z. Fodor and A. Ukawa, *The Endpoint of the first order phase transition of the SU(2) gauge Higgs model on a four-dimensional isotropic lattice*, *Phys. Rev.* **D60** (1999) 013001, [hep-lat/9901021].

[17] M. S. Carena, M. Quiros and C. Wagner, *Electroweak baryogenesis and Higgs and stop searches at LEP and the Tevatron*, *Nucl.Phys.* **B524** (1998) 3–22, [`hep-ph/9710401`].

[18] ATLAS collaboration, G. Aad et al., *Search for top squark pair production in final states with one isolated lepton, jets, and missing transverse momentum in $\sqrt{s} =$8 TeV pp collisions with the ATLAS detector*, *JHEP* **11** (2014) 118, [`1407.0583`].

[19] CMS collaboration, *Search for top squarks decaying to a charm quark and a neutralino in events with a jet and missing transverse momentum*, Tech. Rep. CMS-PAS-SUS-13-009, CERN, Geneva, 2014.

[20] ATLAS collaboration, G. Aad et al., *Search for pair-produced third-generation squarks decaying via charm quarks or in compressed supersymmetric scenarios in pp collisions at $\sqrt{s} = 8$ TeV with the ATLAS detector*, *Phys. Rev.* **D90** (2014) 052008, [`1407.0608`].

[21] CMS collaboration, S. Chatrchyan et al., *Search for top-squark pair production in the single-lepton final state in pp collisions at $\sqrt{s} = 8$ TeV*, *Eur. Phys. J.* **C73** (2013) 2677, [`1308.1586`].

[22] CMS collaboration, V. Khachatryan et al., *Searches for third-generation squark production in fully hadronic final states in proton-proton collisions at $\sqrt{s} = 8$ TeV*, *JHEP* **06** (2015) 116, [`1503.08037`].

[23] A. Katz, M. Perelstein, M. J. Ramsey-Musolf and P. Winslow, *Stop-Catalyzed Baryogenesis Beyond the MSSM*, `1509.02934`.

[24] D. Curtin, P. Jaiswal and P. Meade, *Excluding Electroweak Baryogenesis in the MSSM*, *JHEP* **08** (2012) 005, [`1203.2932`].

[25] W. Huang, J. Shu and Y. Zhang, *On the Higgs Fit and Electroweak Phase Transition*, *JHEP* **1303** (2013) 164, [`1210.0906`].

[26] A. Katz and M. Perelstein, *Higgs Couplings and Electroweak Phase Transition*, *JHEP* **1407** (2014) 108, [`1401.1827`].

[27] S. Profumo, M. J. Ramsey-Musolf, C. L. Wainwright and P. Winslow, *Singlet-Catalyzed Electroweak Phase Transitions and Precision Higgs Studies*, `1407.5342`.

[28] J. R. Espinosa, T. Konstandin and F. Riva, *Strong Electroweak Phase Transitions in the Standard Model with a Singlet*, *Nucl.Phys.* **B854** (2012) 592–630, [`1107.5441`].

[29] P. H. Damgaard, D. O'Connell, T. C. Petersen and A. Tranberg, *Constraints on New Physics from Baryogenesis and Large Hadron Collider Data*, *Phys.Rev.Lett.* **111** (2013) 221804, [`1305.4362`].

[30] D. Curtin, P. Meade and C.-T. Yu, *Testing Electroweak Baryogenesis with Future Colliders*, `1409.0005`.

[31] A. Menon, D. Morrissey and C. Wagner, *Electroweak baryogenesis and dark matter in the nMSSM*, *Phys.Rev.* **D70** (2004) 035005, [`hep-ph/0404184`].

[32] J. Kozaczuk, S. Profumo, L. S. Haskins and C. L. Wainwright, *Cosmological Phase Transitions and their Properties in the NMSSM*, `1407.4134`.

[33] H. H. Patel and M. J. Ramsey-Musolf, *Stepping Into Electroweak Symmetry Breaking: Phase Transitions and Higgs Phenomenology*, *Phys.Rev.* **D88** (2013) 035013, [`1212.5652`].

[34] S. Inoue, G. Ovanesyan and M. J. Ramsey-Musolf, *Two-Step Electroweak Baryogenesis*, 1508.05404.

[35] N. Blinov, J. Kozaczuk, D. E. Morrissey and C. Tamarit, *Electroweak Baryogenesis from Exotic Electroweak Symmetry Breaking*, *Phys. Rev.* **D92** (2015) 035012, [1504.05195].

[36] G. Dorsch, S. Huber and J. No, *A strong electroweak phase transition in the 2HDM after LHC8*, *JHEP* **1310** (2013) 029, [1305.6610].

[37] G. Dorsch, S. Huber, K. Mimasu and J. No, *Echoes of the Electroweak Phase Transition: Discovering a second Higgs doublet through $A_0 \to H_0 Z$*, 1405.5537.

[38] C. Delaunay, C. Grojean and J. D. Wells, *Dynamics of Non-renormalizable Electroweak Symmetry Breaking*, *JHEP* **0804** (2008) 029, [0711.2511].

[39] B. Grinstein and M. Trott, *Electroweak Baryogenesis with a Pseudo-Goldstone Higgs*, *Phys.Rev.* **D78** (2008) 075022, [0806.1971].

[40] C. Grojean, G. Servant and J. D. Wells, *First-order electroweak phase transition in the standard model with a low cutoff*, *Phys.Rev.* **D71** (2005) 036001, [hep-ph/0407019].

[41] B. Henning, X. Lu and H. Murayama, *What do precision Higgs measurements buy us?*, 1404.1058.

[42] D. Bodeker, L. Fromme, S. J. Huber and M. Seniuch, *The Baryon asymmetry in the standard model with a low cut-off*, *JHEP* **02** (2005) 026, [hep-ph/0412366].

[43] V. Barger, P. Langacker, M. McCaskey, M. J. Ramsey-Musolf and G. Shaughnessy, *LHC Phenomenology of an Extended Standard Model with a Real Scalar Singlet*, *Phys. Rev.* **D77** (2008) 035005, [0706.4311].

[44] X.-G. He and J. Tandean, *Low-Mass Dark-Matter Hint from CDMS II, Higgs Boson at the LHC, and Darkon Models*, *Phys. Rev.* **D88** (2013) 013020, [1304.6058].

[45] J. M. Cline, K. Kainulainen, P. Scott and C. Weniger, *Update on scalar singlet dark matter*, *Phys. Rev.* **D88** (2013) 055025, [1306.4710].

[46] F. Kahlhoefer and J. McDonald, *WIMP Dark Matter and Unitarity-Conserving Inflation via a Gauge Singlet Scalar*, *JCAP* **1511** (2015) 015, [1507.03600].

[47] L. Feng, S. Profumo and L. Ubaldi, *Closing in on singlet scalar dark matter: LUX, invisible Higgs decays and gamma-ray lines*, *JHEP* **03** (2015) 045, [1412.1105].

[48] M. Gonderinger, Y. Li, H. Patel and M. J. Ramsey-Musolf, *Vacuum Stability, Perturbativity, and Scalar Singlet Dark Matter*, *JHEP* **01** (2010) 053, [0910.3167].

[49] ATLAS collaboration, G. Aad et al., *Constraints on new phenomena via Higgs boson couplings and invisible decays with the ATLAS detector*, 1509.00672.

[50] CMS collaboration, V. Khachatryan et al., *Precise determination of the mass of the Higgs boson and tests of compatibility of its couplings with the standard model predictions using proton collisions at 7 and 8 TeV*, *Eur. Phys. J.* **C75** (2015) 212, [1412.8662].

[51] V. Barger, P. Langacker, M. McCaskey, M. Ramsey-Musolf and G. Shaughnessy, *Complex Singlet Extension of the Standard Model*, *Phys.Rev.* **D79** (2009) 015018, [0811.0393].

[52] M. Gonderinger, H. Lim and M. J. Ramsey-Musolf, *Complex Scalar Singlet Dark Matter: Vacuum Stability and Phenomenology*, *Phys.Rev.* **D86** (2012) 043511, [`1202.1316`].

[53] M. Jiang, L. Bian, W. Huang and J. Shu, *Impact of a complex singlet: From dark matter to baryogenesis*, `1502.07574`.

[54] A. Drozd, B. Grzadkowski, J. F. Gunion and Y. Jiang, *Extending two-Higgs-doublet models by a singlet scalar field - the Case for Dark Matter*, *JHEP* **11** (2014) 105, [`1408.2106`].

[55] M. Cirelli, N. Fornengo and A. Strumia, *Minimal dark matter*, *Nucl. Phys.* **B753** (2006) 178–194, [`hep-ph/0512090`].

[56] M. Cirelli, A. Strumia and M. Tamburini, *Cosmology and Astrophysics of Minimal Dark Matter*, *Nucl. Phys.* **B787** (2007) 152–175, [`0706.4071`].

[57] T. Hambye, F. S. Ling, L. Lopez Honorez and J. Rocher, *Scalar Multiplet Dark Matter*, *JHEP* **07** (2009) 090, [`0903.4010`].

[58] P. Fileviez Perez, H. H. Patel, M. Ramsey-Musolf and K. Wang, *Triplet Scalars and Dark Matter at the LHC*, *Phys.Rev.* **D79** (2009) 055024, [`0811.3957`].

[59] CMS collaboration, V. Khachatryan et al., *Search for disappearing tracks in proton-proton collisions at $\sqrt{s} = 8$ TeV*, *JHEP* **01** (2015) 096, [`1411.6006`].

[60] W. Chao and M. J. Ramsey-Musolf, *Electroweak Baryogenesis, Electric Dipole Moments, and Higgs Diphoton Decays*, *JHEP* **10** (2014) 180, [`1406.0517`].

[61] W. Chao and M. J. Ramsey-Musolf, *Catalysis of Electroweak Baryogenesis via Fermionic Higgs Portal Dark Matter*, `1503.00028`.

[62] M. A. Fedderke, J.-Y. Chen, E. W. Kolb and L.-T. Wang, *The Fermionic Dark Matter Higgs Portal: an effective field theory approach*, *JHEP* **08** (2014) 122, [`1404.2283`].

[63] D. G. E. Walker, *Unitarity Constraints on Higgs Portals*, `1310.1083`.

[64] D. Curtin, R. Essig, S. Gori and J. Shelton, *Illuminating Dark Photons with High-Energy Colliders*, *JHEP* **02** (2015) 157, [`1412.0018`].

[65] A. Noble and M. Perelstein, *Higgs self-coupling as a probe of electroweak phase transition*, *Phys.Rev.* **D78** (2008) 063518, [`0711.3018`].

[66] CMS collaboration, *Higgs pair production at the High Luminosity LHC*, Tech. Rep. CMS-PAS-FTR-15-002, CERN, Geneva, 2015.

[67] *Prospects for measuring Higgs pair production in the channel $H(\to \gamma\gamma)H(\to b\bar{b})$ using the ATLAS detector at the HL-LHC*, Tech. Rep. ATL-PHYS-PUB-2014-019, CERN, Geneva, Oct, 2014.

[68] *Higgs Pair Production in the $H(\to \tau\tau)H(\to b\bar{b})$ channel at the High-Luminosity LHC*, Tech. Rep. ATL-PHYS-PUB-2015-046, CERN, Geneva, Nov, 2015.

[69] K. Fujii et al., *Physics Case for the International Linear Collider*, `1506.05992`.

[70] A. J. Barr, M. J. Dolan, C. Englert, D. E. Ferreira de Lima and M. Spannowsky, *Higgs Self-Coupling Measurements at a 100 TeV Hadron Collider*, *JHEP* **02** (2015) 016, [`1412.7154`].

[71] A. Azatov, R. Contino, G. Panico and M. Son, *Effective field theory analysis of double Higgs boson production via gluon fusion*, *Phys. Rev.* **D92** (2015) 035001, [`1502.00539`].

[72] C. Englert and M. McCullough, *Modified Higgs Sectors and NLO Associated Production*, *JHEP* **07** (2013) 168, [1303.1526].

[73] M. McCullough, *An Indirect Model-Dependent Probe of the Higgs Self-Coupling*, *Phys. Rev.* **D90** (2014) 015001, [1312.3322].

[74] M. Gorbahn, J. M. No and V. Sanz, *Benchmarks for Higgs Effective Theory: Extended Higgs Sectors*, *JHEP* **10** (2015) 036, [1502.07352].

[75] CMS collaboration, *Projected Performance of an Upgraded CMS Detector at the LHC and HL-LHC: Contribution to the Snowmass Process*, in *Community Summer Study 2013: Snowmass on the Mississippi (CSS2013) Minneapolis, MN, USA, July 29-August 6, 2013*, 2013. 1307.7135.

[76] *Projections for measurements of Higgs boson signal strengths and coupling parameters with the ATLAS detector at a HL-LHC*, Tech. Rep. ATL-PHYS-PUB-2014-016, CERN, Geneva, Oct, 2014.

[77] "CEPC Pre-CDR." http://cepc.ihep.ac.cn/preCDR/main_preCDR.pdf.

[78] TLEP Design Study Working Group collaboration, M. Bicer et al., *First Look at the Physics Case of TLEP*, *JHEP* **01** (2014) 164, [1308.6176].

[79] ATLAS collaboration, ATLAS Collaboration, *Search for neutral Higgs bosons of the minimal supersymmetric standard model in pp collisions at $\sqrt{s}$ = 8 TeV with the ATLAS detector*, *JHEP* **11** (2014) 056, [1409.6064].

[80] CMS collaboration, *Search for charged Higgs bosons with the H+ to tau nu decay channel in the fully hadronic final state at sqrt s = 8 TeV*, .

[81] CMS collaboration, S. Chatrchyan et al., *Search for a Higgs boson decaying into a b-quark pair and produced in association with b quarks in proton-proton collisions at 7 TeV*, *Phys.Lett.* **B722** (2013) 207–232, [1302.2892].

[82] ATLAS collaboration, G. Aad et al., *Search for Higgs bosons in Two-Higgs-Doublet models in the $H \to WW \to e\nu\mu\nu$ channel with the ATLAS detector*, Tech. Rep. ATLAS-CONF-2013-027, CERN, Geneva, Mar, 2013.

[83] CMS collaboration, V. Khachatryan et al., *Searches for heavy Higgs bosons in two-Higgs-doublet models and for $t \to ch$ decay using multilepton and diphoton final states in pp collisions at 8 TeV*, *Phys. Rev.* **D90** (2014) 112013, [1410.2751].

[84] G. Aad et al., *Search for charged Higgs bosons in the τ+jets final state with pp collision data recorded at $\sqrt{s} = 8$ TeV with the ATLAS experiment*, Tech. Rep. ATLAS-CONF-2013-090, CERN, Geneva, Aug, 2013.

[85] CMS collaboration, S. Chatrchyan et al., *Higgs to tau tau (MSSM)*, Tech. Rep. CMS-PAS-HIG-13-021, CERN, Geneva, 2013.

[86] CMS collaboration, CMS Collaboration, *Search for a Charged Higgs Boson in pp Collisions at $\sqrt{s} = 8$ TeV*, *JHEP* **11** (2015) 018, [1508.07774].

[87] ATLAS collaboration, ATLAS Collaboration, *Search for charged Higgs bosons decaying via $H^{\pm} \to \tau^{\pm}\nu$ in fully hadronic final states using pp collision data at $\sqrt{s} = 8$ TeV with the ATLAS detector*, *JHEP* **03** (2015) 088, [1412.6663].

[88] CMS collaboration, CMS Collaboration, *Search for neutral MSSM Higgs bosons decaying to a pair of tau leptons in pp collisions*, *JHEP* **10** (2014) 160, [`1408.3316`].

[89] S. Dawson et al., *Working Group Report: Higgs Boson*, in *Community Summer Study 2013: Snowmass on the Mississippi (CSS2013) Minneapolis, MN, USA, July 29-August 6, 2013*, 2013. `1310.8361`.

[90] B. Coleppa, F. Kling and S. Su, *Exotic Higgs Decay via AZ/HZ Channel: a Snowmass Whitepaper*, `1308.6201`.

[91] B. Coleppa, F. Kling and S. Su, *Exotic Decays Of A Heavy Neutral Higgs Through HZ/AZ Channel*, *JHEP* **1409** (2014) 161, [`1404.1922`].

[92] E. Brownson, N. Craig, U. Heintz, G. Kukartsev, M. Narain et al., *Heavy Higgs Scalars at Future Hadron Colliders (A Snowmass Whitepaper)*, `1308.6334`.

[93] B. Coleppa, F. Kling and S. Su, *Charged Higgs search via $AW^{\pm}/HW^{\pm}$ channel*, *JHEP* **1412** (2014) 148, [`1408.4119`].

[94] F. Kling, A. Pyarelal and S. Su, *Light Charged Higgs Bosons to AW/HW via Top Decay*, `1504.06624`.

[95] T. Li and S. Su, *Exotic Higgs Decay via Charged Higgs*, `1504.04381`.

[96] U. Maitra, B. Mukhopadhyaya, S. Nandi, S. K. Rai and A. Shivaji, *Searching for an elusive charged Higgs boson at the Large Hadron Collider*, *Phys.Rev.* **D89** (2014) 055024, [`1401.1775`].

[97] L. Basso, A. Lipniacka, F. Mahmoudi, S. Moretti, P. Osland et al., *Probing the charged Higgs boson at the LHC in the CP-violating type-II 2HDM*, *JHEP* **1211** (2012) 011, [`1205.6569`].

[98] R. Dermisek, J. P. Hall, E. Lunghi and S. Shin, *A New Avenue to Charged Higgs Discovery in Multi-Higgs Models*, *JHEP* **1404** (2014) 140, [`1311.7208`].

[99] B. Mohn, N. Gollub and K. A. Assamagan, *The ATLAS discovery potential for a heavy Charged Higgs boson in a large mass splitting MSSM scenario*, Tech. Rep. ATL-PHYS-PUB-2005-017. ATL-COM-PHYS-2005-021., CERN, Geneva, 2005.

[100] K. Assamagan, *Signature of the charged Higgs decay H+- to W h0 with the ATLAS detector*, *Acta Phys.Polon.* **B31** (2000) 881–893.

[101] K. A. Assamagan, Y. Coadou and A. Deandrea, *ATLAS discovery potential for a heavy charged Higgs boson*, *Eur.Phys.J.direct* **C4** (2002) 9, [`hep-ph/0203121`].

[102] ATLAS collaboration, ATLAS Collaboration, *Searches for Higgs boson pair production in the $hh \to bb\tau\tau, \gamma\gamma WW*, \gamma\gamma bb, bbbb$ channels with the ATLAS detector*, *Phys. Rev.* **D92** (2015) 092004, [`1509.04670`].

[103] ATLAS collaboration, ATLAS Collaboration, *Search for Higgs boson pair production in the $b\bar{b}b\bar{b}$ final state from pp collisions at $\sqrt{s} = 8$ TeV with the ATLAS detector*, *Eur. Phys. J.* **C75** (2015) 412, [`1506.00285`].

[104] ATLAS collaboration, ATLAS Collaboration, *Search For Higgs Boson Pair Production in the $\gamma\gamma b\bar{b}$ Final State using pp Collision Data at $\sqrt{s} = 8$ TeV from the ATLAS Detector*, *Phys. Rev. Lett.* **114** (2015) 081802, [`1406.5053`].

[105] CMS collaboration, CMS Collaboration, *Search for resonant pair production of Higgs bosons decaying to two bottom quarkantiquark pairs in protonproton collisions at 8 TeV*, *Phys. Lett.* **B749** (2015) 560–582, [1503.04114].

[106] CMS collaboration, *Search for a pseudoscalar boson A decaying into a Z and an h boson in the llbb final state*, Tech. Rep. CMS-PAS-HIG-14-011, CERN, Geneva, 2014.

[107] ATLAS collaboration, ATLAS Collaboration, *Search for a CP-odd Higgs boson decaying to Zh in pp collisions at $\sqrt{s} = 8$ TeV with the ATLAS detector*, *Phys. Lett.* **B744** (2015) 163–183, [1502.04478].

[108] CMS collaboration, *Search for H/A decaying into Z+A/H, with Z to ll and A/H to fermion pair*, Tech. Rep. CMS-PAS-HIG-15-001, CERN, Geneva, 2015.

[109] CMS collaboration, CMS Collaboration, *Search for a pseudoscalar boson decaying into a Z boson and the 125 GeV Higgs boson in $l^+l^-b\bar{b}$ final states*, *Phys. Lett.* **B748** (2015) 221–243, [1504.04710].

[110] J. Hajer, Y.-Y. Li, T. Liu and J. F. H. Shiu, *Heavy Higgs Bosons at 14 TeV and 100 TeV*, *JHEP* **11** (2015) 124, [1504.07617].

[111] J. M. No and M. Ramsey-Musolf, *Probing the Higgs Portal at the LHC Through Resonant di-Higgs Production*, *Phys.Rev.* **D89** (2014) 095031, [1310.6035].

[112] M. J. Dolan, C. Englert and M. Spannowsky, *Higgs self-coupling measurements at the LHC*, *JHEP* **1210** (2012) 112, [1206.5001].

[113] C.-Y. Chen, S. Dawson and I. M. Lewis, *Exploring resonant di-Higgs boson production in the Higgs singlet model*, *Phys. Rev.* **D91** (2015) 035015, [1410.5488].

[114] V. Barger, L. L. Everett, C. B. Jackson, A. D. Peterson and G. Shaughnessy, *New physics in resonant production of Higgs boson pairs*, *Phys. Rev. Lett.* **114** (2015) 011801, [1408.0003].

[115] M. J. Dolan, C. Englert and M. Spannowsky, *New Physics in LHC Higgs boson pair production*, *Phys. Rev.* **D87** (2013) 055002, [1210.8166].

Scenario	BSM DOF	EWPT	DM	Collider Signatures
Real Singlet	1	Tree-level single-step or two-step	X	∗ Two neutral mixed states ∗ Modified trilinear self-coupling ∗ Reduced SM-like signal strength ∗ Resonant di-Higgs production w/ final states: $b\bar{b}\tau^{+}\tau^{-}$, $b\bar{b}\gamma\gamma$ etc. ∗ Exotic decays: $f\bar{f}\gamma\gamma$ etc.
Real Singlet	1	X	$\sqrt{}$	∗ Invisible Higgs decays
Real Singlet	1	Two-step Loop-induced one-step	$\sqrt{}$	∗ VBF $h^{*} \to$ invisible ∗ Modified trilinear self-coupling
Complex Singlet	2	Tree-level single-step	$\sqrt{}$	∗ Two neutral mixed states plus scalar DM ∗ Modified trilinear self-coupling ∗ Reduced SM-like signal strength ∗ Resonant di-Higgs production w/ final states: $b\bar{b}\tau^{+}\tau^{-}$, $b\bar{b}\gamma\gamma$ etc. ∗ Exotic decays: $f\bar{f}\gamma\gamma$ etc. ∗ Invisible decays
Real Triplet	3	Loop-induced multi-step	$\sqrt{}$	∗ Reduced $\Gamma(h \to \gamma\gamma)$ ∗ Disappearing charged particle tracks
Real Triplet	3	Loop-induced multi-step	X	∗ Reduced $\Gamma(h \to \gamma\gamma)$ ∗ EW $H^{\pm}H^{\mp}$ and $H^{\pm}H^{0}$ production w/ novel final states: $b\bar{b}\tau\nu$, $b\bar{b}W^{\pm}Z$, etc.
2HDM	4	Loop-induced single step	X	$A^{0} \to Z^{0}H^{0}$
Higher-dim operators	0	Tree-level single-step	X	

Table 1. Higgs portal scenarios. For each scenario, the number of additional BSM degrees of freedom (DOF) is indicated, along with the nature of the EWPT and viability as a contributor to the dark matter (DM) relic density. The quantity $\sqrt{}$ (X) indicates viable (not viable). The final column summarizes the possible collider signatures for each scenario.

	Decay	Final States	Channels
Neutral Higgs H^{0}, A	HH type	$(bb/\tau\tau/WW/ZZ/\gamma\gamma)(bb/\tau\tau/WW/ZZ/\gamma\gamma)$	$H^{0} \to AA$, ...
	HZ type	$(\ell\ell/qq/\nu\nu)(bb/\tau\tau/WW/ZZ/\gamma\gamma)$	$H^{0} \to AZ, A \to H^{0}Z$, ...
	$H^{+}H^{-}$ type	$(tb/\tau\nu/cs)(tb/\tau\nu/cs)$	$H^{0} \to H^{+}H^{-}$, ...
	$H^{\pm}W^{\mp}$ type	$(\ell\nu/qq')(tb/\tau\nu/cs)$	$H^{0}/A \to H^{\pm}W^{\mp}$, ...
Charged Higgs	$HW^{\pm}$ type	$(\ell\nu/qq')(bb/\tau\tau/WW/ZZ/\gamma\gamma)$	$H^{\pm} \to H^{0}W, AW$, ...

Table 2. Exotic decay modes for Higgses in the 2HDM with the heavy Higgs boson decays to two light Higgses or one light Higgs boson with one SM gauge boson. H in column two refers to any of the neutral Higgs bosons h^{0}, H^{0} or A.

Scenario	Conditions	Collider	Signatures	Ref.
Real Singlet	EWPT	LHC	Signal reduction	[11, 27, 43]
		ILC, FCC-ee,	Signal reduction	[11, 27]
		CEPC, SppC/FCC-hh		
	EWPT	LHC	Modified self-coupling	[11, 26, 27, 65]
		ILC, TLEP	Modified self-coupling	[27]
		CEPC, SppC/FCC-hh		
	EWPT	LHC	$h_2 \to h_1 h_1 \to b\bar{b}\tau^+\tau^-$	[111]
			$h_2 \to h_1 h_1 \to b\bar{b}\gamma\gamma$	[113, 114]
			$h_2 \to h_1 h_1 \to b\bar{b}b\bar{b}$	[113]
			$h_2 \to h_1 h_1 \to b\bar{b}VV$	In prog
			$h_1 \to h_2 h_2 \to XY$	In prog
Real Singlet	DM	LHC	Invisible decays	[30, 43, 44]
Real Singlet	DM* & EWPT	SppC/FCC-hh	VBF $h_1^* \to$ invis	[30]
			invisible decays	
			modified self-coupling	
		ILC/FCC-ee/CEPC	modified self-coupling	[30]
			Signal reduction	
Real Triplet	EWPT & DM*	LHC	Disappearing charged particle tracks	[58]
			Reduced $\Gamma(h \to \gamma\gamma)$	[33]
Real Triplet	EWPT only	LHC	Reduced $\Gamma(h \to \gamma\gamma)$	[33]
			$H^+ H_2^0 \to b\bar{b}\tau\nu$	[58]
	EWPT only		$H^+ H_2^0 \to H_2^0 H_2^0 \pi^+$	
			$H^+ H^- \to H_2^0 H_2^0 \pi^+ \pi^-$	
			with	
			$H_2^0 H_2^0 \to b\bar{b}\gamma\gamma$	[58]
			$H_2^0 H_2^0 \to b\bar{b}\tau^+\tau^-$	
2HDM	EWPT	LHC	$A^0 \to ZH^0 \to \ell\ell b\bar{b}$	[37]
			$A^0 \to ZH^0 \to \ell\ell W^+ W^-$	[37]

Table 3. Higgs portal scenarios signatures. For each scenario, the cosmological relevance is indicated in the second column. The third column gives the collider for which the signature indicated in the fourth column has been analyzed. The final column gives appropriate references. For exotic Higgs boson decays, see Table 2. * For this case, we do not assume saturation of the DM relic density.